

REMARKS

The Examiner's reconsideration of the application is urged in view of the amendment above and comments which follow.

Taking the matters raised by the Examiner in turn, another copy of the MATSUMOTO reference is submitted herewith. It is believed that a copy was submitted with the IDS, and may have been misplaced by the Patent and Trademark Office.

In numbered Sections 4 and 5 of the office action, the Examiner has objected to the specification because the abstract is not on a separate sheet (although it is part of the published international document), and the disclosure has a formatting problem. Regarding the abstract, an appropriate abstract is appended hereto. Regarding the specification, the copy possessed by the undersigned does not have the numbering problem, nor did the published international application. A substitute specification is submitted herewith, and is identical to the published international specification. Nothing has been added. Should anything further be required, it is requested that the Examiner contact the undersigned.

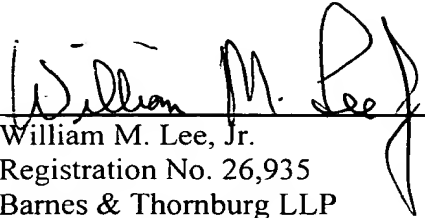
In numbered Section 7 of the office action, the Examiner has rejected claims 26-30 and 35-62 under 35 U.S.C. Section 112 as being indefinite. With the amendments above, it is believed that the matters raised by the Examiner have been properly rectified and the claims are now in proper form.

The Examiner's indication of the allowability of the claims is gratefully acknowledged. The applicant has no comments concerning the reasons for allowance, and given the above and the attachments hereto, it is believed that the application is now fully in condition for allowance and such further action by the Examiner is solicited.

Further and favorable reconsideration of the application is therefore urged.

April 30, 2004

Respectfully submitted,

A handwritten signature in black ink, appearing to read "William M. Lee, Jr.", is written over a horizontal line.

William M. Lee, Jr.
Registration No. 26,935
Barnes & Thornburg LLP
P.O. Box 2786
Chicago, Illinois 60690-2786
(312) 214-4800
(312) 759-5646 (fax)

This Page Is Inserted by IFW Operations
and is not a part of the Official Record

BEST AVAILABLE IMAGES

Defective images within this document are accurate representations of the original documents submitted by the applicant.

Defects in the images may include (but are not limited to):

- BLACK BORDERS
- TEXT CUT OFF AT TOP, BOTTOM OR SIDES
- FADED TEXT
- ILLEGIBLE TEXT
- SKEWED/SLANTED IMAGES
- COLORED PHOTOS
- BLACK OR VERY BLACK AND WHITE DARK PHOTOS
- GRAY SCALE DOCUMENTS

IMAGES ARE BEST AVAILABLE COPY.

**As rescanning documents *will not* correct images,
please do not report the images to the
Image Problems Mailbox.**



INVITED PAPER Special Issue on Mobile Communications

Combined Convolutional Coding/Diversity Reception for QDPSK Land Mobile Radio

Tadashi MATSUMOTO† and Fumiyuki ADACHI†, Members

SUMMARY Diversity combining and error correction coding are powerful means to combat the multipath fading encountered in mobile radio communications. In this paper, we theoretically analyze the joint effects of postdetection diversity combining and convolutional coding with soft decision Viterbi decoding for QDPSK signal transmissions. The union bounding formula is used for average BER performance calculation taking into account the additive white Gaussian noise (AWGN), co-channel interference, and multipath channel delay spread. Symbol puncturing is applied to produce higher rate codes from original 1/2-rate convolutional codes. Numerical calculations are presented for the required average signal energy per bit-to-noise power spectrum density ratio (E_b/N_0), required average signal-to-interference power ratio (SIR) and tolerable rms delay spread needed to achieve a certain average BER. Spectrum efficiency of cellular systems is also calculated.

1. Introduction

Nyquist filtered quaternary differential phase shift keying (QDPSK) is a bandwidth efficient modulation scheme and is attractive for land mobile radio applications^{(1),(2)}. Mobile radio channels suffer from multipath fading caused by reflection of the transmitted signals by nearby buildings and other obstacles⁽³⁾. Diversity combining and error correction coding are the most powerful techniques to combat multipath fading. Postdetection diversity is attractive for mobile radio use⁽⁴⁾⁻⁽⁶⁾ because it does not require any cophas-ing function (predetection diversity reception does) which is difficult to achieve in fast fading channels. Reference(10) shows that soft decision Viterbi decoding of convolutional codes⁽⁷⁾⁻⁽⁹⁾ is equivalent to post-detection diversity reception. Thus, if it is combined with diversity reception, BER performance can be significantly improved. So far, however, the effects of diversity reception and convolutional coding have been analyzed independently. The aim of this paper is to analyze the joint effects of postdetection diversity combining and convolutional coding with soft decision Viterbi decoding for QDPSK signal transmissions. Sect. 2 presents overview of postdetection diversity combining and convolutional coding. The analysis of average BER performance is presented in Sect. 3, taking into account additive white Gaussian noise

(AWGN), cochannel interference, and multipath channel delay spread. Symbol puncturing is applied to produce higher rate codes from the original 1/2-rate convolutional code. Numerical calculations are shown in Sect. 4 for the required average signal energy per bit-to-noise power spectrum density ratio (E_b/N_0), required average signal-to-interference power ratio (SIR) and tolerable delay spread for a certain average BER. Spectrum efficiency of cellular systems is also calculated.

2. Overview of Diversity Combining and Error Correction Coding

Diversity reception requires multiple antennas. Basically, there are two types of diversity reception, i.e., predetection and postdetection diversity. Predetection diversity reception cophas and combines all the received signals before signal detection. The cophas-ing function is, however, difficult to achieve because of rapid phase variations due to multipath fading. Since all the detector outputs are in phase, postdetection diversity reception requires no cophas-ing function and hence is attractive for mobile radio use. Adachi et al.⁽⁴⁾⁻⁽⁶⁾ analyzed its performance for digital FM and QDPSK signal transmissions. Postdetection diversity combining weights each detector output so that the contribution of diversity branches with weak signals are reduced. The combiner output of D -branch diversity can be represented as

$$v(t) = \sum_{d=1}^D w_d(t) v_d(t), \quad (1)$$

where $v_d(t)$ is the detector output of d -th branch ($d = 1, 2, \dots, D$) and $w_d(t)$ is the weighting factor. The best performance is obtained when $w_d(t) = R_d^2(t)$, where $R_d(t)$ is the d -th branch detector input envelope. This diversity combining is referred to as post-detection maximal-ratio combining (MRC) because it is analogous to predetection MRC⁽⁶⁾. Postdetection MRC diversity was also analyzed for QDPSK in Ref. (11).

Present cellular mobile radio systems employ short BCH codes. However convolutional coding has attracted much attention recently, since soft decision Viterbi decoding can provide more powerful error correction

capability than hard decision decoding of the block codes. Divsalar and Simon⁽⁹⁾ investigated trellis coded MPSK for fading channels. Matsumoto and Adachi⁽¹⁰⁾ recently investigated the effect of soft decision Viterbi decoding taking into account cochannel interference. It was shown that the optimal code design criteria is to maximize the length of the shortest error event path length and the phase product along the path. It was also shown that soft decision Viterbi decoding is equivalent to postdetection MRC diversity. Hence, the combination of diversity reception and convolutional coding can yield significant performance improvements. However, there has been no analysis of the combined effects of diversity reception and convolutional coding, except for hard decision decoding of BCH codes⁽¹²⁾.

3. Ber Analysis

(A) Transmission system

The overall transmission system is shown in Fig. 1. The input bit stream is encoded by a 1/2-rate convolutional coder, and its output symbol sequence (a_m, b_m) , $m = \dots -1, 0, 1, \dots$, is then block-interleaved symbol by symbol to obtain the interleaved symbol sequence (a_n, b_n) , $n = \dots -1, 0, 1, \dots$. We assume that the interleaving degree is large enough so that the fading variations associated with each symbol in the deinterleaved symbol sequence can be considered statistically independent. The modulation scheme assumed here is QDPSK, where the symbol to be transmitted is mapped to the differential phase $\Delta\phi_n = \phi_n - \phi_{n-1}$ of the carrier. $\Delta\phi_n$ is given by

$$\Delta\phi_n = \begin{cases} 3\pi/2 & (a_n, b_n) = (-1, 1) \\ \pi & (1, 1) \\ \pi/2 & (1, -1) \\ 0 & (-1, -1) \end{cases} \quad (2)$$

To achieve intersymbol interference (ISI) free transmission and a narrowband spectrum, we use a Nyquist raised cosine transfer function for overall filter response, which is shared equally between transmitter and receiver. Overall impulse response is

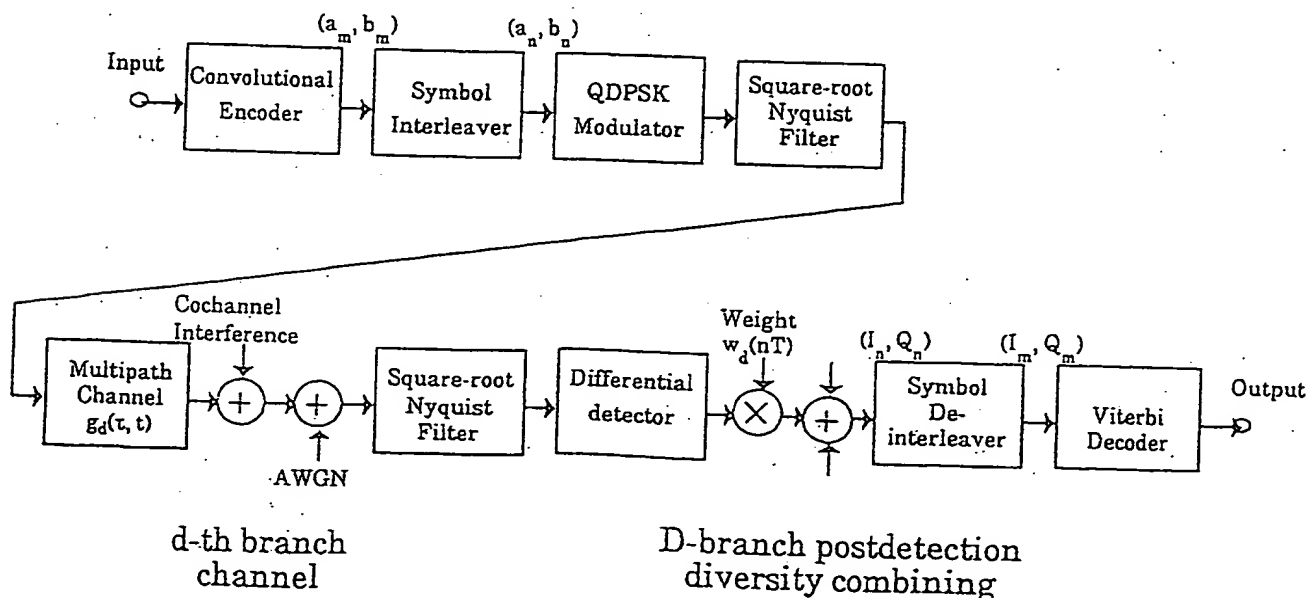
$$h(t) = \frac{\sin(\pi t/T) \cos(a\pi t/T)}{\pi t/T \cdot 1 - (2at/T)^2}, \quad (3)$$

where T is the symbol duration, and a is the roll-off factor ($0 \leq a \leq 1$).

Signal transmission between mobile and base stations takes place over multipath channels. We assume that fading is much slower than the symbol rate so that the multipath channel transfer function remains almost constant over several symbols. The input to the d -th branch detector ($d=1, 2, \dots, D$) of the D -branch postdetection diversity receiver can be written using the complex envelope representation as

$$\begin{aligned} z_d(t) &= z_{sd}(t) + z_{id}(t) + z_{nd}(t) \\ &= \int_{-\infty}^{\infty} s(t-\tau) g_d(\tau, t) d\tau + z_{id}(t) + z_{nd}(t), \end{aligned} \quad (4)$$

where $s(t)$ is the desired signal component without fading, $g_d(\tau, t)$ is the baseband equivalent multipath



channel impulse response (measured from the instant of application of a unit impulse at t), $z_{id}(t)$ is the cochannel interference, and $z_{nd}(t)$ is the bandwidth restricted AWGN component with one-sided spectrum density N_0 . $s(t)$ is the overall response of the transmitter and receiver filters to the QDPSK signal and is given by

$$s(t) = \sqrt{\frac{2E_s}{T}} d_R(t) = \sqrt{\frac{2E_s}{T}} \sum_{n=-\infty}^{\infty} e^{j\phi_n} h(t-nT), \quad (5)$$

where E_s is the average signal energy per symbol. Since the impulse response at τ is due to the sum of many independent impulses caused by reflections from buildings and other obstacles, $g_d(\tau, t)$ can be assumed to be a zero-mean complex Gaussian process of t , and the delay-time correlation function can be given by

$$\langle g_d(\tau, t) g_d^*(\tau-\lambda, t-\mu) \rangle = \xi_s(\tau, \mu) \delta(\lambda), \quad (6)$$

for $d=1, 2, \dots, D$,

where the asterisk denotes complex conjugate, $\delta(\cdot)$ is the delta function. $\xi_s(\tau, 0)$ is called the delay profile. The rms delay spread τ_{rms} is the important factor that determines the average BER under frequency selective fading. τ_{rms} is defined as

$$\tau_{rms} = \sqrt{\int_{-\infty}^{\infty} (\tau - \tau_{mean})^2 \xi_s(\tau, 0) d\tau} \quad (7)$$

$$\tau_{mean} = \int_{-\infty}^{\infty} \tau \xi_s(\tau, 0) d\tau,$$

where τ_{mean} is the mean time delay and $\int \xi_s(\tau, 0) d\tau = 1$.

Differential detection is assumed. A quadrature differential detector output of the d -th branch can be represented in the complex form as

$$v_d(t) = I_d(t) + jQ_d(t) \\ = e^{j\pi/4} \frac{z_d(t) z_d^*(t-T)}{|z_d(t)| |z_d(t-T)|} \quad (8)$$

The D differential detector outputs are weighted and combined using postdetection MRC. The weighting factor $w_d(nT)$ for differential detection is $|z_d(nT)| |z_d^*((n-1)T)|$, which is approximately equal to $R_d^2(nT)$. The combiner output at the sampling instant $t=nT$ becomes

$$I(nT) + jQ(nT) = e^{j\pi/4} \sum_{d=1}^D z_d(nT) z_d^*((n-1)T). \quad (9)$$

The de-interleaver output sequence is $I(mT) + jQ(mT)$. The Viterbi decoder calculates the path metric l which is the sum of the branch metric l_m , i.e., $l = \sum l_m$, along the path to select the symbol sequence with the greatest path metric value at each path merge. The

branch metric for the m -th symbol

$$l_m = R_e[-(a'_m + jb'_m)\{I(mT) + jQ(mT)\}^*] \\ = -a'_m I(mT) - b'_m Q(mT) \quad (10)$$

can be used for differential detection^{(10),(13)}, where (a'_m, b'_m) is the m -th symbol in a possible sequence. Since Gray coding is assumed in Eq. (2), the linear property of the algebraic convolutional code structure is maintained in the QDPSK signal space. Hence, we assume that codeword X_0 with an all zero $(-1, -1)$ symbol sequence is transmitted. X_0 corresponds to an all-zero state path in the trellis diagram. The i -th opposing codeword $X_{k,i}$ whose path diverges from the all zero-state path and merges with it after k symbols. The transmitted codeword survives if path metric of X_0 is larger than that of $X_{k,i}$. Otherwise, the opposing codeword $X_{k,i}$ survives. We introduce the differential path metric Δl defined as

$$\Delta l = \left[\sum_{(a'_m, b'_m)=(1,1)} \{I(mT) + Q(mT)\} \right. \\ \left. + \sum_{(a'_m, b'_m)=(1,-1)} I(mT) + \sum_{(a'_m, b'_m)=(-1,1)} Q(mT) \right], \quad (11)$$

where the opposing codeword survives if $\Delta l < 0$. We assume that the numbers of symbols $(a'_m, b'_m) = (1, 1)$, $(1, -1)$, and $(-1, 1)$ in the opposing path are L , M , and N , respectively.

(B) Upper bound

The probability of an incorrect path being selected can be calculated from the probability distribution function (pdf) of Δl . The average BER after decoding can be upper-bounded by the union-bound formula as⁽¹⁰⁾

$$P_b \leq \sum_{k=K}^{\infty} \sum_{i=1}^{N_k} n_{k,i} P_{k,i}, \quad (12)$$

where $P_{k,i}$ is the average survival probability of $X_{k,i}$, $n_{k,i}$ is the number of error bits when the opposing codeword $X_{k,i}$ is selected, N_k is the number of the opposing codewords with length k , and K is the constraint length. The high rate codes are obtained by periodically deleting some symbols from the original convolutional coder output (symbol puncturing)⁽¹⁴⁾. $p-1$ symbols among $2p$ symbols of the original code sequence are periodically deleted to produce a $p/(p+1)$ -rate code. The average BER can be also upper-bounded by

$$P_b \leq \frac{1}{2p} \sum_{k=K}^{\infty} \sum_{i=1}^{N_k} n_{k,i} P_{k,i} \quad (13)$$

where N_k is the number of all possible opposing paths with length k , which diverge from the all zero state path during the puncturing period $2p$.

$I(mT)$ and $Q(mT)$ are the real part and imagi-

nary part of the sum of $z_d(mT) \times z_d^*((m-1)T)$, $d = 1, \dots, D$. Since we are assuming perfect interleaving, fading associated with each symbol in the path is independent, and thus, the differential path metric Δl given by Eq. (11) becomes the sum of independent Gaussian variables when all $z_d(mT)$'s are given. The BER analysis described in Ref. (6) can be applied to obtain the average survival probability.

The conditional survival probability $p_{ki} = \text{Prob}[\Delta l < 0 | \text{all } z_d(mT) \text{'s being given}]$ is given by

$$p_{ki} = \frac{1}{2} \text{erfc} \left[\frac{\rho_c}{\sqrt{1 - |\rho|^2}} \frac{R}{\sqrt{2}\sigma} \right]. \quad (14)$$

R is given by

$$R = \sqrt{\sum_{d=1}^D \left[2 \sum_{(a_m, b_m)=(1,1)} |z_d(mT)|^2 + \sum_{(a_m, b_m)=(1,-1)} |z_d(mT)|^2 + \sum_{(a_m, b_m)=(-1,1)} |z_d(mT)|^2 \right]} \quad (15)$$

$\rho = \rho_c + j\rho_s = (1/2) \langle z_d(mT) \cdot z_d^*((m-1)T) \rangle / \sigma^2$ with $\sigma^2 = (1/2) \langle |z_d(mT)|^2 \rangle = (1/2) \langle |z_d(m-1)T|^2 \rangle$ and is given by

$$\begin{aligned} \rho &= e^{j\pi/4} \\ &\cdot 2\Gamma \int_{-\infty}^{\infty} \xi_s(\tau, T) d_R(-\tau) d_R^*(-T-\tau) d\tau \\ &+ \Gamma/\Lambda \int_{-\infty}^{\infty} \xi_i(\tau, T) d_i(-\tau) d_i(-T-\tau) d\tau \\ &/ \left\{ \sqrt{2\Gamma \int_{-\infty}^{\infty} \xi_s(\tau, 0) |d_R(-\tau)|^2 d\tau} \right. \\ &\cdot \left. + \Gamma/\Lambda \int_{-\infty}^{\infty} \xi_i(\tau, 0) |d_i(-\tau)|^2 d\tau + 1 \right\} \\ &\times \left\{ \sqrt{2\Gamma \int_{-\infty}^{\infty} \xi_s(\tau, 0) |d_R(-T-\tau)|^2 d\tau} \right. \\ &\cdot \left. + \Gamma/\Lambda \int_{-\infty}^{\infty} \xi_i(\tau, 0) |d_i(-T-\tau)|^2 d\tau + 1 \right\} \end{aligned} \quad (16)$$

where Γ and Λ are the average E_b/N_0 and the average SIR, respectively. $d_R(t)$ and $d_i(t)$ are the overall filter responses to the desired and cochannel interference signals, respectively, and $d_R(t)$ is shown in Eq. (5).

To calculate ρ under frequency selective fading, the ISI from adjacent symbols must be taken into account. In this paper, we assume one adjacent symbol on each side because the rms delay spreads are much smaller than the symbol duration being considered. We have assumed that cochannel interference modulation

caused when desired signal fades and the modulation timing difference is not important). $d_i(t)$ is identical to $d_R(t)$ except that (a_m, b_m) are replaced by the interference symbol sequence.

In deriving Eq. (14), we have assumed that ρ_c and ρ_s are identical. In cochannel interference environments and with frequency selective fading, however, this does not hold. The case $\rho_c = \rho_s$ happens when the cochannel interference symbol is (1, 1) and when the desired signal adjacent symbols are $(a_{m-1}, b_{m-1}) = (a_{m+1}, b_{m+1}) = (1, 1)$ under frequency selective fading. This is the worst case in the sense that the average BER is largest.

The conditional survival probability p_{ki} dominates for small values of R . This suggests that the average survival probability P_{ki} can be calculated using approximate pdf of R for small values of R . We are assuming perfect symbol interleaving and that D fading signals are mutually independent. It can be seen from Eq. (15) that since $z_d(mT)$ is the complex Gaussian variable, R^2 is the sum of $D \times L$ independent exponential variables with mean $2\sigma^2$ and $D \times (M+N)$ independent exponential variables with mean σ^2 . A derivation of the approximate pdf of R can be found in Ref. (18). Since

$$p(R) \approx \frac{1}{2^{DL}} \frac{1}{\{D(L+M+N)-1\}!} \cdot \frac{R^{2D(L+M+N)-1}}{2^{D(L+M+N)-1} \sigma^{2D(L+M+N)}}, \quad (17)$$

we have

$$\begin{aligned} p_{ki} &\approx \int_0^\infty p_{ki} \cdot p(R) dR \\ &\approx \frac{1}{2^{DL+1}} \frac{\{2D(L+M+N)-1\}!!}{\{D(L+M+N)\}!} \\ &\cdot \left\{ \frac{1 - |\rho|^2}{2\rho_c^2} \right\}^{D(L+M+N)} \end{aligned} \quad (18)$$

(C) Discussions

Causes of bit errors are AWGN, cochannel interference, random FM noise, and multipath channel delay spreads. Delay spreads place an upper limit on the bit rate, hence it is a very important factor for designing high speed digital systems. Cochannel interference performance is also important for cellular systems because the same radio frequency must be reused at different cells⁽³⁾. Average BERs can be approximately represented as the sum of four parts⁽³⁾, i.e., those due to AWGN, cochannel interference, random FM noise, and delay spreads. Upper bound for the average BER is given by Eqs. (12) and (13). In the following, we present the individual average survival probabilities to provide a good insight into BER.

are

$$P_{ki} \approx \frac{1}{2^{DL+1}} \frac{\{2D(L+M+N)-1\}!!}{\{D(L+M+N)\}!} \left(\frac{1}{\Gamma}\right)^{D(L+M+N)} \quad (\text{AWGN}) \quad (19)$$

$$P_{ki} \approx \frac{1}{2^{DL+1}} \frac{\{2D(L+M+N)-1\}!!}{\{D(L+M+N)\}!} \left(\frac{4}{\Lambda}\right)^{D(L+M+N)} \quad (\text{cochannel interference}) \quad (20)$$

$$P_{ki} \approx \frac{1}{2^{DL+1}} \frac{\{2D(L+M+N)-1\}!!}{\{D(L+M+N)\}!} \cdot \left\{2\pi f_{rms} T\right\}^{2D(L+M+N)} \quad (\text{random FM noise}) \quad (21)$$

$$P_{ki} \approx \frac{1}{2^{DL+1}} \frac{\{2D(L+M+N)-1\}!!}{\{D(L+M+N)\}!} \cdot \left\{T \mid d'_R(0) d_R(-T) - d_R(0) d'_R(-T) \mid \cdot \left(\frac{\tau_{rms}}{T}\right)^{2D(L+M+N)} \right\} \quad (\text{delay spread}) \quad (22)$$

where f_{rms} is the rms Doppler frequency and the prime denotes time derivative.

The parameter which dominates the survival probability is the value of $D \times (L+M+N)$, i.e., the product of diversity order (the number of diversity branches) and the shortest error event path length of the codes. Increasing the diversity order by more than two is not practical because of the limited space for diversity antennas, especially in hand-held portables. On the contrary, codes with a large $L+M+N$ value are difficult to achieve when Viterbi decoder complexity is restricted (for example, a decoder with more than 64 states is impractical for hand-held portables because of its large power consumption). However, the combination of convolutional coding with Viterbi decoding provides equivalent $D \times (L+M+N)$ -branch diversity reception. Thus, joint use of diversity combining and convolutional coding is more practical than simply increasing diversity order or choosing a lower code rate to increase the $L+M+N$ value.

Reference (9) has shown that the design criteria for the optimal codes is to maximize the length of the shortest error event path length (maximize the smallest $L+M+N$ value) and the phase product (2^L). It is found from Eqs. (19)-(22) that as the value of $D \times (L+M+N)$ increases, the error rate drops rapidly in inverse-proportion to the $D \times (L+M+N)$ -th power of Γ , Λ , f_{rms} , T or τ_{rms}/T . Also, the average BER decreases inversely in proportion to 2^L . Therefore, the optimal design for the codes with diversity reception in fading channels is to maximize the value of $D \times (L+M+N)$, and the phase product. However, for large

values of $D \times (L+M+N)$, the phase product is not important.

4. Numerical Calculation

We can calculate the upper bound for average BER using Eqs. (12) and (13). Individual results are

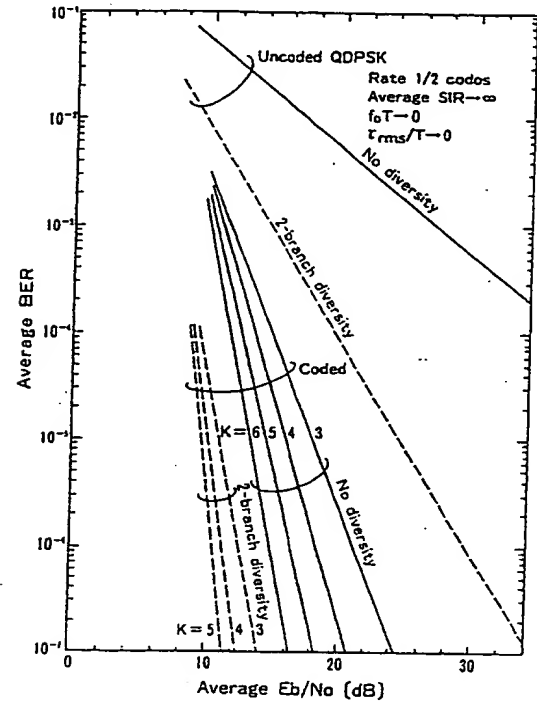


Fig. 2 Average BER due to AWGN.

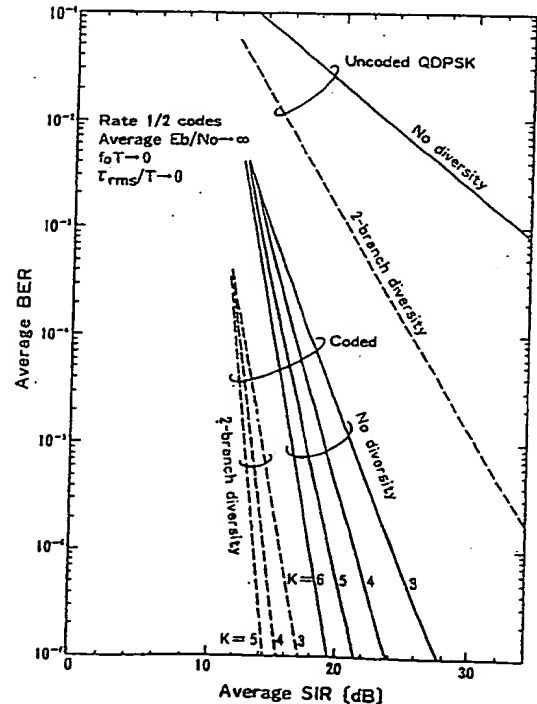


Fig. 3 Average BER due to cochannel interference.

presented for the average BERs due to AWGN, cochannel interference, random FM noise, and delay spread.
(A) 1/2-Rate convolutional codes.

Figures 2-4 show BER performances due to AWGN, cochannel interference, and random FM noise. When calculating the BER performance due to random FM noise, we assumed that equal amplitude

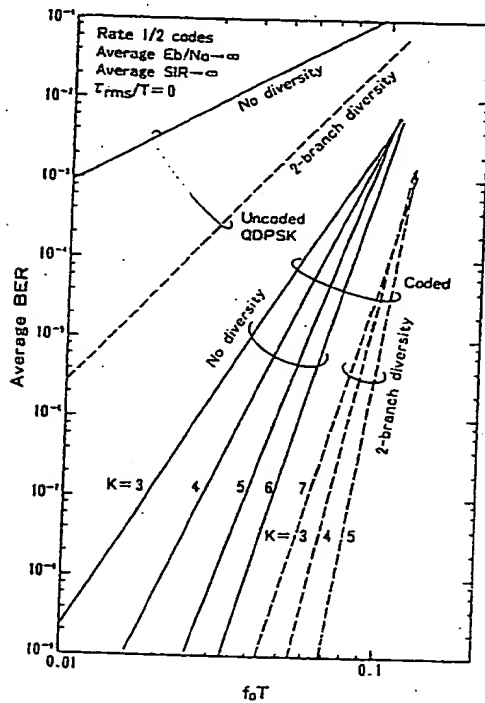


Fig. 4 Average BER due to random FM noise.

multipath waves arrive from all directions with equal probability, thus, $\xi_s(\mu) = J_0(2\pi f_D \mu)$, where $J_0(\cdot)$ is the Bessel function and $f_D (= \sqrt{2}f_{rms})$ is the maximum Doppler frequency given by vehicle speed/carrier wavelength.

Table 1 shows the generator polynomials⁽¹⁴⁾ of the codes used here. Gain of the combined diversity reception/coding (combined gain) is defined as the reduction in average E_b/N_0 necessary for achieving a certain BER. It is found from Fig. 2 that as the constraint length K increases, the improvement in average BER becomes larger. When diversity reception is not used, the coding gain at $BER=10^{-4}$ is increased by about 3.2dB as K increases from 3 to 6. However, with two-branch diversity reception, the combined gain increase is only about 0.8 dB. This result suggests that with two-branch diversity reception, the $K=3$ code, whose decoder complexity is 1/8-th that of $K=6$ code, can be used. This is an important finding of practical significance. A similar result is found for cochannel interference performance.

The random FM noise places a lower limit on achievable BER. Even if $K=3$, the code reduces the average BER considerably. Without diversity reception, the tolerable value of $f_D T$ for $BER=10^{-6}$ is about 0.025. Diversity reception with $D=2$ increases this value to $f_D T=0.07$. This suggests that for a symbol rate ($=1/T$) of 21 ksymbol/sec and 900 MHz carrier frequency, if the vehicle velocity is less than 1760 km/hour, $BER \leq 10^{-6}$ can be achieved.

Table 1 Generator polynomials (octal notation) of the 1/2-rate convolutional codes and optimal deletion positions for their symbol punctured codes.

K	Code Rate					
	1/2(Original Code)	2/3	3/4	4/5	5/6	6/7
	Generator Polynomial	Optimum Deletion Position				
3	5, 7	0111	011011	—	—	
4	15, 17			01101011		
5	23, 35			01010111	0101101101	0101010111011
6	53, 75					
7	133, 171					

Symbols whose positions are indicated as "1" are deleted.

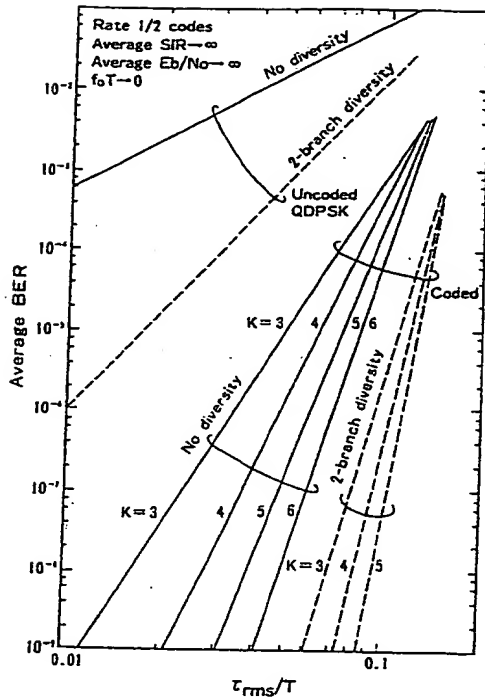


Fig. 5 Average BER due to delay spread.

Figure 5 shows the average BER versus normalized rms delay spread. For small values of normalized delay spread, the shape of the delay profile is of no importance⁽⁶⁾. Double-spike delay profile is assumed. For $K=3$ code, if an average BER of 10^{-6} is required, two-branch ($D=2$) diversity can increase the tolerable normalized delay spread by about two-fold (from $\tau_{rms}/T=0.05$ to 0.12). For a symbol rate of 21 ksymbol/sec, the tolerable rms delay spread is, without diversity and coding, less than $0.5 \mu\text{sec}$. If $K=3$ code is used without diversity, the tolerable value is $\tau_{rms} \leq 2 \mu\text{sec}$. Two-branch diversity increases this value to $\tau_{rms} \leq 6 \mu\text{sec}$. This indicates the great advantage of using combined diversity and coding.

(B) Punctured codes

The optimal deleted symbol positions to minimize the BER after decoding were found by computer search for $p=2 \sim 6^{(10)}$ assuming no cochannel interference and no delay spread. The search results for the optimal symbol positions are listed in Table 1. Combined coding gains in E_b/N_0 at $\text{BER}=10^{-4}$ versus code rate for $K=5$ codes are plotted in Fig. 6. $f_0T \rightarrow 0$ and $\text{SIR} \rightarrow \infty$ are assumed. When diversity reception is used, the combined coding gain decreases less rapidly than that without diversity. For a given channel bandwidth, a higher information bit rate can be achieved with only a slight increase in the required E_b/N_0 .

Figure 7 shows the tolerable rms delay spread normalized by the information symbol rate for $K=5$ punctured codes assuming $\text{BER}=10^{-4}$. Since channel coding expands the radio channel bit rate by a factor of $(\text{code rate})^{-1}$, the effect of delay spread becomes more

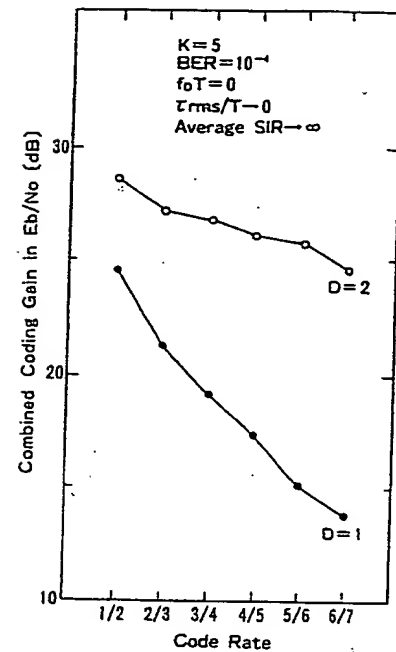
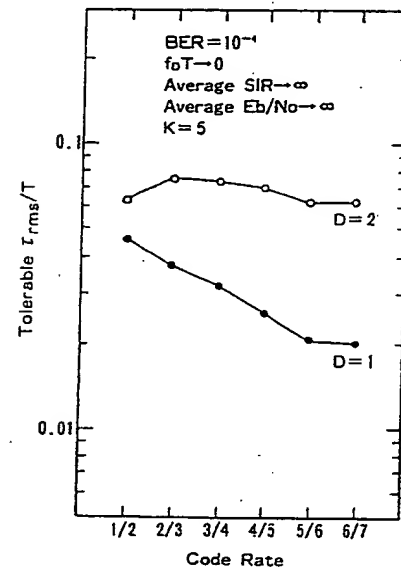
Fig. 6 Combined coding gain in E_b/N_0 at average $\text{BER}=10^{-4}$.

Fig. 7 Tolerable normalized rms delay spread.

severe. However, error correction capability increases as the code rate decreases. It is found from Fig. 7 that if diversity reception is not used, the tolerable τ_{rms}/T value is largest with the rate 1/2 code, and decreases rapidly with higher code rates. If two-branch diversity is used, the largest tolerable τ_{rms}/T value is about 0.75 which is achieved for the code with rate 2/3. However, with two-branch diversity, the tolerable τ_{rms}/T value is less sensitive to the code rate. Therefore, high rate codes can yield almost the largest tolerable τ_{rms}/T value with relatively small channel bandwidth expansion. This suggests the use of the rate 6/7 code.

Figure 8 shows the combined coding gains in the cochannel interference limited channel. It is found

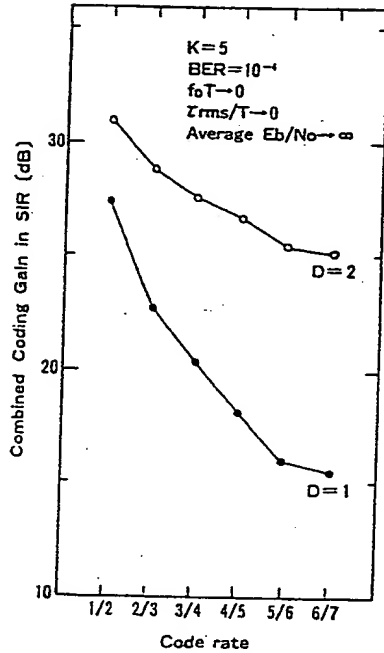


Fig. 8 Combined coding gain in SIR at average BER=10⁻⁴.

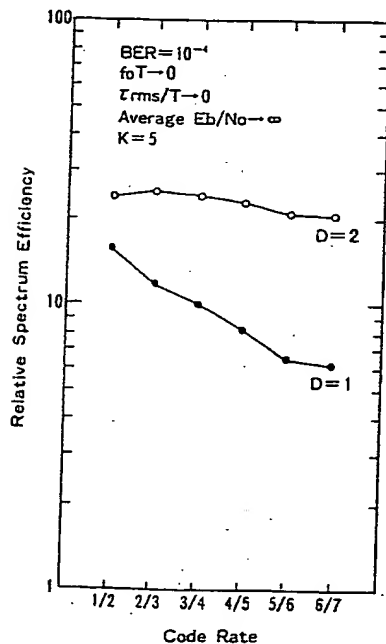


Fig. 9 Spectrum efficiency.

from this figure that the decrease in the SIR coding gain is similar to that in the E_b/N_0 coding gain. It should be noted that when the information bit rate is kept constant, as the code rate increases, the radio channel bit rate decreases, and thus, the number of channels available within a given bandwidth increases. Cellular systems reuse the same radio frequency at spatially different cells. Spectrum efficiency η of cellular system was calculated assuming hexagonal cell

$$\eta \propto r \{1 + (\alpha \Lambda_{th})^{1/\alpha}\}^{-2}, \quad (23)$$

where α is the propagation constant (typical value for urban area is $\alpha=3.5^{(15)}$), α is the margin for the allowable probability Q of geographical outage at the cell fringe due to shadow fading, and Λ_{th} is the required average SIR for achieving the specified BER. Assuming log-normal shadow fading with a standard deviation δ (in dB), $Q=1/2 \operatorname{erfc}(\alpha/2\delta)$. The values of Λ_{th} can be obtained from Fig. 8. Assuming that the specified BER is 10^{-4} for a data communication as an example, calculated spectrum efficiencies normalized by that with no diversity and no coding, and the results are shown in Fig. 9 for $K=5$ codes. When diversity reception is used, the optimum code rate that maximizes the spectrum efficiency is around 2/3. Moreover, with diversity reception, the spectrum efficiency is less sensitive to the code rate than that without diversity. Therefore, for a given channel bandwidth, a higher rate code can be used to achieve higher information bit rates with only a slight sacrifice in spectrum efficiency.

5. Conclusion

This paper has analyzed the joint effects of post-detection diversity combining and convolutional coding with Viterbi decoding in mobile radio multipath fading channels for QPSK signal transmission. Combined coding gains in average E_b/N_0 and SIR, tolerable rms delay spread, and spectrum efficiency of cellular systems, were calculated. Without diversity, performance degrades as the code rate increases because the shortest error event path length decreases. When diversity reception with $D=2$ is employed (two-branch diversity is considered to be the most practical), however, the tolerable rms delay spread and the spectrum efficiency are relatively insensitive to the code rate. This paper considered QPSK modulation scheme. The TDMA cellular systems currently being developed in Japan and North America are to employ $\pi/4$ -shift QPSK^{(16),(17)}. Both modulation schemes have identical spectra. The difference is the mapping rule of the transmitted symbols to the differential phase of the carrier. Despite of the different mapping rules, both modulation schemes provide almost identical BER performance (BER due to AWGN is identical)⁽⁵⁾. Hence, the results presented in this paper can be applied to systems employing $\pi/4$ -shift QPSK.

References

- (1) Jenks F. G., Morgan P. D. and Warren C. S.: "Use of four-level phase modulation for digital mobile radio", IEEE Trans. Electromagn. Compat., EMC-14, pp. 113-128 (Nov. 1972).
- (2) Akaiwa Y. and Nagata Y.: "Highly efficient digital

- 895 (June 1987).
- (3) ed. Jakes W. C. Jr.: "Microwave Mobile Communications", Wiley, New York (1974).
 - (4) Ohno K. and Adachi F.: "Effects of postdetection selection diversity reception in QDPSK land mobile radio", *Electron. Lett.*, 25, pp. 1293-1294 (Sept. 1989).
 - (5) Adachi F. and Ohno K.: "BER performance of QDPSK with postdetection diversity reception in mobile radio channels", *IEEE Trans. Veh. Technol.*, 40, 1 (Feb. 1991).
 - (6) Adachi F. and Parsons J. D.: "Error rate performance of digital FM mobile radio with postdetection diversity", *IEEE Trans. Commun.*, 37, pp. 200-210 (March 1989).
 - (7) Modestino J. W. and Mui S. Y.: "Convolutional code performance in the Rican fading channel", *IEEE Trans. Commun.*, COM-24, pp. 592-606 (June 1976).
 - (8) Hagenauer J. and Lutz E.: "Forward error correction coding for fading compensation in mobile satellite channels", *IEEE J. Sel. Areas Commun.*, SAC-5, pp. 215-225 (Feb. 1987).
 - (9) Divsalar D. and Simon M. K.: "The design of trellis coded MPSK for fading channel: performance criteria", *IEEE Trans. Commun.*, COM-36, pp. 1004-1012 (Sept. 1988).
 - (10) Matsumoto T. and Adachi F.: "BER analysis of convolutional coded QDPSK in digital mobile radio", *IEEE Trans. Veh. Technol.*, to be published.
 - (11) Horikoshi J.: "Error performance improvement of QDPSK in the presence of cochannel or multipath interference using diversity", *Trans. IECE Japan*, J67-B, pp. 24-31 (Jan. 1984).
 - (12) Adachi F. and Suda H.: "Effects of diversity reception on BCH-coded QPSK cellular land mobile radio", *Electron. Lett.*, 25, pp. 188-189 (Feb. 1989).
 - (13) Rainish D. and Perl J. M.: "Generalized cutoff rate of time- and frequency-selective fading channels", *IEEE Trans. Commun.*, COM-37, pp. 449-467 (May 1989).
 - (14) Yasuda Y., Kashiki K. and Hirata Y.: "High-rate punctured convolutional codes for soft decision Viterbi decoding", *IEEE Trans. Commun.*, COM-32, pp. 315-319 (March 1984).
 - (15) Okumara Y., Ohmori E., Kawano T. and Fukuda K.: "Field strength and its variability in VHF and UHF land mobile radio service", *Rev. Elec. Commun. Lab.*, pp. 825-873 (Sept.-Oct. 1968).
 - (16) Uddenfeldt J. Rith K. and Hedberg B.: "Digital technologies in cellular radio", *Proc. 38th IEEE VTC*, pp. 516-519, Philadelphia (June 15-17 1989).
 - (17) "Special Issue on Digital mobile telephone system", *J. IEICE*, 73, pp. 804-808 (Aug. 1990).
 - (18) Shwartz M., Bennett W. and Stein S.: "Communication Systems and Techniques", McGraw-Hill, New York (1966).



Tadashi Matsumoto received the B. S. and M. S. degrees in electrical engineering from Keio University, Japan, in 1978 and 1980, respectively. He was awarded a Doctorate in Engineering from the same university in 1991. He is a senior research engineer of NTT Radio Communication Systems Laboratories, Yokosuka-shi. Since joining NTT in 1980, he participated in R&D project of NTT's High Capacity Mobile Communication System up to 1987. Since May 1987, he has been researching digital mobile radio systems. His current interest is in error control strategies such as FEC and/or ARQ for mobile radio channels. He is currently involved in the development of data communication systems for TDMA cellular mobile radios. Dr. Matsumoto is a member of the IEEE.



Fumiyuki Adachi graduated from Tohoku University, Japan in 1973 and was awarded a Doctorate in Engineering from the same University in 1984. Since 1973 he has been with Nippon Telegraph & Telephone Corporation (NTT) Laboratories. Presently, he is a research group leader for mobile communication signal processing, including modulation/demodulation, diversity reception, channel coding, and is deeply involved in the development of TDMA cellular mobile radio systems. During the academic year of 1984/85, he was a United Kingdom SERC Visiting Research Fellow at the Department of Electrical Engineering and Electronics of Liverpool University. He is a co-recipient of the IEEE Vehicular Technology Society 1980 Paper of the Year Award. Dr. Adachi is a member of the IEEE.